Journal of Macromolecular Science, Part A
Publication details, including instructions for authors and subscription information:
http://www.informaworld.com/smpp/title~content=t713597274

Study on Self-assembly of Poly(ethylene glycol)- *block*-poly(γ-benzyl *L*-glutamate)-*graft*-poly(ethylene glycol) Copolymer and Poly(γ-benzyl *L*-glutamate)- *block*-poly(ethylene glycol) Copolymer in Ethanol

Guo-Quan Zhu[a]
[a] School of Materials Science and Engineering, Shandong University of Technology, Zibo, P.R. China

To cite this Article Zhu, Guo-Quan(2009) 'Study on Self-assembly of Poly(ethylene glycol)- *block*-poly(γ-benzyl *L*-glutamate)-*graft*-poly(ethylene glycol) Copolymer and Poly(γ-benzyl *L*-glutamate)- *block*-poly(ethylene glycol) Copolymer in Ethanol', Journal of Macromolecular Science, Part A, 46: 9, 892 — 898
To link to this Article: DOI: 10.1080/10601320903078313
URL: http://dx.doi.org/10.1080/10601320903078313

Journal of Macromolecular Science®, Part A: Pure and Applied Chemistry (2009) **46**, 892–898

ISSN: 1060-1325 print / 1520-5738 online
DOI: 10.1080/10601320903078313

Taylor & Francis
Taylor & Francis Group

Study on Self-assembly of Poly(ethylene glycol)-*block*-poly(γ-benzyl *L*-glutamate)-*graft*-poly(ethylene glycol) Copolymer and Poly(γ-benzyl *L*-glutamate)-*block*-poly(ethylene glycol) Copolymer in Ethanol

GUO-QUAN ZHU

School of Materials Science and Engineering, Shandong University of Technology, Zibo 255049, P.R. China.

Received January 2009, Accepted March 2009

Poly(ethylene glycol)-*block*-poly(γ-benzyl *L*-glutamate)-*graft*-poly(ethylene glycol) (PEG-*b*-PBLG-*g*-PEG) copolymer was synthesized by the ester exchange reaction of poly(γ-benzyl *L*-glutamate)-*block*-poly(ethylene glycol) (PBLG-*block*-PEG) copolymer with PEG chain, and PBLG-*block*-PEG copolymer was prepared by a standard *N*-carboxyl-γ-benzyl-*L*-glutamate anhydride (NCA) method. Nuclear magnetic resonance (NMR) spectroscopy was used to confirm the components of PBLG-*block*-PEG and PEG-*b*-PBLG-*g*-PEG. The self-association behaviors of PBLG-*block*-PEG and PEG-*b*-PBLG-*g*-PEG in ethanol were investigated by transmission electron microscopy (TEM), dynamic laser scattering (DLS), and viscometry. The experimental results revealed that the different molecular structures could exert marked effects on the self-assembly behaviors of PBLG-*block*-PEG and PEG-*b*-PBLG-*g*-PEG in ethanol. PBLG-*block*-PEG and PEG-*b*-PBLG-*g*-PEG could self-assemble to form polymeric micelles with a core-shell structure in the shapes of plump spherical and regular rice-like, respectively. Effects of the introduction of PBLG homopolymer on the average particle diameter of the micelles of PBLG-*block*-PEG and PEG-*b*-PBLG-*g*-PEG and influence of testing temperature on the critical micelle concentration of different copolymers were studied.

Keywords: Poly(γ-benzyl *L*-glutamate)-*block*-poly(ethylene glycol), poly(ethylene glycol)-*block*-poly(γ-benzyl *L*-glutamate)-*graft*-poly(ethylene glycol), self-assembly, molecular structure, morphology

1 Introduction

In the past decade, self-assembly of amphiphilic copolymers in selective solvents has received much attention both experimentally and theoretically (1–40). Due to their amphiphilic characteristics, copolymers with hydrophobic and hydrophilic components can self-assemble to form micelles or nanoparticles with a core-shell structure (1). The nanoscale structure holds a range of potential applications such as carriers of catalysts, protein simulation, macromolecular conformational study, drug delivery system, nanoreactors, etc. (1–15).

Relative to other amphiphilic copolymers, polypeptide amphiphilic copolymers have received much attention for self-assembly and biopolymeric characteristics. Kwon et al. reported that poly(β-benzyl *L*-aspartate) (PBLA)/poly(ethylene oxide) (PEO) diblock copolymers could self-assemble to form polymeric micelles composed of an outer shell of PEO and an inner core of PBLA in aqueous medium (26). Cho et al. have reported the formation of polymeric micelles composed of poly(γ-benzyl *L*-glutamate) and poly(ethylene oxide) in aqueous medium and the drug delivery system based on the core-shell nanoparticles with PBLG as the hydrophobic inner core and PEO as the hydrophilic outer shell (22). Harada et al. have studied the relationship between the conformation of the polypeptide chain and the supramolecular structure of poly(*L*-lysine)-*block*-poly(ethylene glycol). It was revealed that the α-helix structure of polypeptide segments tend to be stabilized by the PEG segments through the formation of a dimer with a micelle-like structure in aqueous medium (6).

Compared with pure polypeptide block structure copolymers, polypeptide copolymers with both block structure and graft structure are expected to possess different self-assembly behaviors. To our knowledge, few experimental work has so far been reported on the comparison of the self-assembly behavior of poly(ethylene glycol)-*block*-poly(γ-benzyl *L*-glutamate)-*graft*-poly(ethylene glycol) copolymer

Address correspondence to: Guo-Quan Zhu, School of Materials Science and Engineering, Shandong University of Technology, Zibo 255049, P.R. China. E-mail: guoquanzhu111@163.com

with poly(γ-benzyl L-glutamate)-*block*-poly(ethylene glycol) copolymer in ethanol. In the present work, PEG-*b*-PBLG-*g*-PEG copoymer and PBLG-*block*-PEG copolymer were synthesized. The self-association behaviors of PBLG-*block*-PEG and PEG-*b*-PBLG-*g*-PEG in ethanol were studied by TEM, DLS, and viscometry. The experimental results revealed that the different molecular structures could exert marked effects on the self-assembly behaviors of PBLG-*block*-PEG and PEG-*b*-PBLG-*g*-PEG in ethanol. PBLG-*block*-PEG and PEG-*b*-PBLG-*g*-PEG could self-assemble to form polymeric micelles with a core-shell structure in the shapes of plump spherical and regular rice-like, respectively. Effects of the introduction of PBLG homopolymer on the average particle diameter of the micelles based on PBLG-*block*-PEG and PEG-*b*-PBLG-*g*-PEG and influence of testing temperature on the critical micelle concentration of different copolymers were researched.

2 Experimental

2.1 Materials

The amine-terminated α-methoxy-ω-amino poly(ethylene glycol) (AT-PEG, M_w =5,000 or 20,000) and poly(ethylene glycol methyl ether) (mPEG, M_w =350) were purchased from Sigma Inc., and used without further purification. Hexane, tetrahydrofuran (THF) and 1, 4-dioxane are of analytical grade and dried with sodium to remove water before use. All other solvents are of analytical grade and used without further purification.

2.2 Syntheses of Polypeptide Copolymers

PBLG homopolymer was prepared by a standard *N*-carboxyl-γ-benzyl-*L*-glutamate anhydride (NCA) method (8–10). The molecular weight of the PBLG homopolymer was estimated from the [η] value measured in dichloroacetic acid (DCA) according to the document (41). The molecular weight of PBLG homopolymer used in the study is 20,000.

PBLG-*block*-PEG (shown as Figure 1a) was prepared by a standard *N*-carboxyl-γ-benzyl-*L*-glutamate anhydride (NCA) method (10). Briefly, PBLG-*block*-PEG copolymer was obtained by the ring-opening polymerization of γ-BLG NCA initiated by AT-PEG (M_w = 5,000 or 20,000) in 1, 4-dioxane at room temperature for 72 h. The molecular weight of PBLG-*block*-PEG copolymer was estimated by nuclear magnetic resonance (NMR) measurements (Avance 550). It was calculated by the peak intensities of the methylene proton signal of polypeptide and the ethylene proton signal of PEG in the ^{1}H-NMR spectra (1,10). The molecular weights of PBLG-*block*-PEG1 (AT-PEG, M_w =5,000) and PBLG-*block*-PEG2 (AT-PEG,

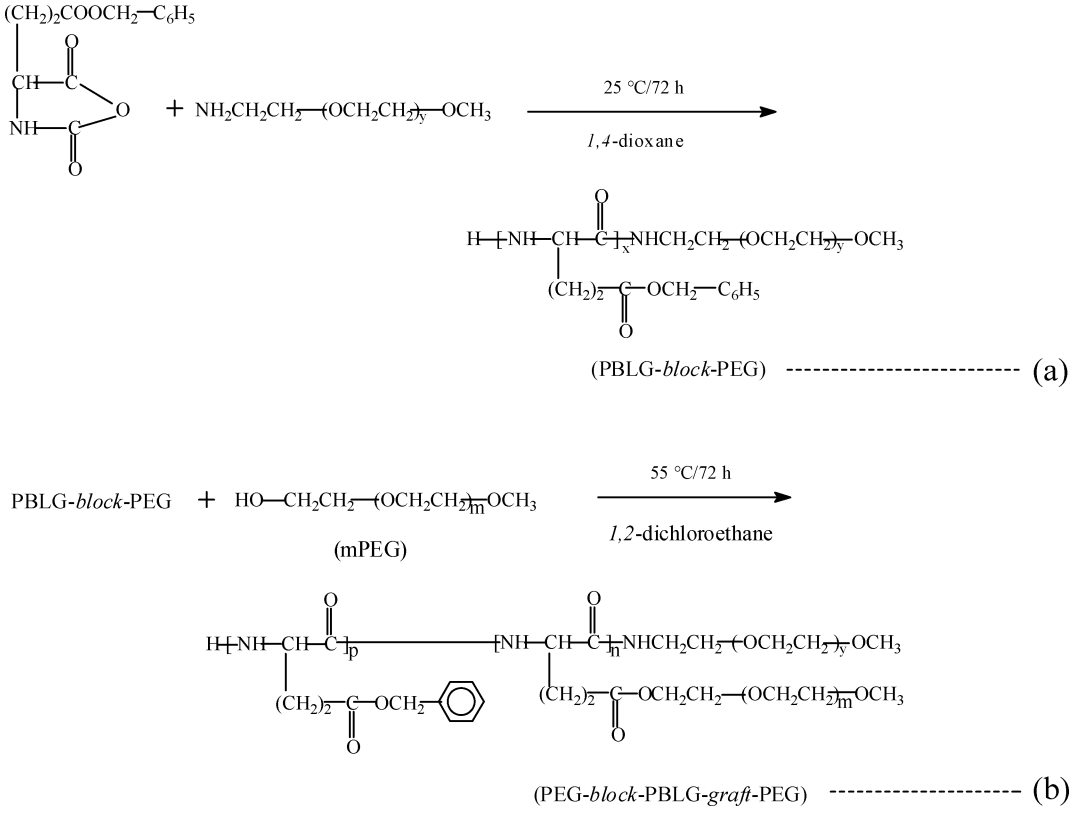

Fig. 1. Synthesis of (a) PBLG-*block*-PEG copolymer and (b) PEG-*b*-PBLG-*g*-PEG copolymer.

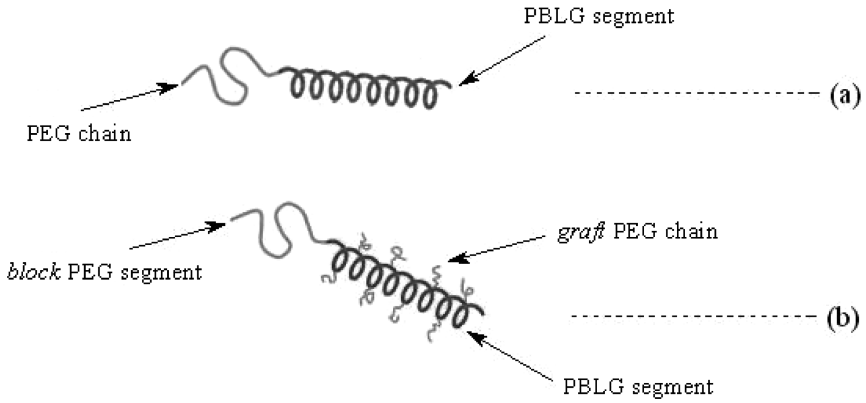

Fig. 2. Schematic representations of (a) PBLG-*block*-PEG copolymer structure and (b) PEG-*b*-PBLG-*g*-PEG copolymer structure.

M_w = 20,000) used in the study are 75,000 and 140,000, respectively.

PEG-*b*-PBLG-*g*-PEG copolymer (shown as Figure 1b) was obtained by the ester exchange reaction of PBLG-*block*-PEG with mPEG (M_w = 350) in 1, 2-dichloroethane with *p*-toluenesulfonic acid as a catalyst according to the method described in the literatures (1, 28–30). The block copolymer used in the study is PBLG-*block*-PEG2, and the corresponding block-graft copolymer synthesized is denoted as PEG-*b*-PBLG-*g*-PEG2. The mixture reacted at 55°C for 72 h and then was precipitated into a large volume of anhydrous ethanol. The resulting product was purified twice by repeated precipitation from a chloroform solution in a large volume of anhydrous methanol, and then dried under vacuum. The grafting ratio of PEG-*b*-PBLG-*g*-PEG2 copolymer was estimated by nuclear magnetic resonance (NMR) measurements (Avance 550). It was calculated by the peak intensities of the methylene proton signal of polypeptide and the ethylene proton signal of PEG in the ^{1}H-NMR spectra (1,10). To emphasize one point, for PEG-*b*-PBLG-*g*-PEG2 copolymer, the peak area ($A_{\delta=3.62}$) used in calculating the grafting ratio is the subtraction of A_1 and A_2 ($A_1 > A_2$), where A_1 (value is 4.96) is the peak area (3.62 ppm) in PEG-*b*-PBLG-*g*-PEG2 spectrum, A_2 (value is 1.66) is the peak area (3.62 ppm) in PBLG-*block*-PEG2 spectrum. From the difference of the peak area (3.62 ppm), the formation of PEG-*b*-PBLG-*g*-PEG2 copolymer was proved. According to the ^{1}H-NMR analysis, the grafting ratio of PEG-*b*-PBLG-*g*-PEG2 copolymer is 17.2%. Figure 2 shows the schematic representations of (a) PBLG-*block*-PEG copolymer structure and (b) PEG-*b*-PBLG-*g*-PEG copolymer structure.

2.3 Preparation of Polypeptide Copolymer Micelles

The obtained polypeptide copolymer samples were first dissolved in $CHCl_3$ to make a 2 g/l polymer solution. Subsequently, a given volume of ethanol was added into the polymer $CHCl_3$ solution with stirring. The formation of the polypeptide copolymer micelles occurred, as indicated by the appearance of turbidity in the solution, when about 20 vol% ethanol was added. After 2 h, the addition of ethanol was continued until the polymer concentration in the micelle solution was about 0.2 g/l (37). The micelle solution was kept overnight and then dialyzed against ethanol using dialysis membranes (3500 molecular weight cut-off) to remove the $CHCl_3$ for 48 h at room temperature. It was preferred that ethanol was exchanged at intervals of 10–12 h. The solution was diluted with ethanol to the desired concentration.

2.4 ^{1}H-NMR Measurements

^{1}H-NMR spectra of PBLG-*block*-PEG2 and PEG-*b*-PBLG-*g*-PEG2 in $CDCl_3$ were measured using a NMR instrument (Avance 550) at 500 MHz.

2.5 Observation of Transmission Electron Microscope

The morphology of the micelles was obtained by TEM (JEM-1200-EXII). Drops of micelle solution were placed on a carbon film coated copper grid, and then were dried at room temperature. Before the observations, the sample was stained by aqueous phosphotungstic acid solution (1.0 wt%). The TEM bright field imaging was performed with 120 kV accelerating voltage.

2.6 Dynamic Laser Scattering Measurements

Dynamic laser scattering (DLS) was measured using a S4700 (Malvern Instrument, UK) with an argon laser beam at a wavelength of 488 nm at 25°C. A scattering angle of 90°C was used. The concentration of the sample was 0.1 g/l in ethanol and the sample was filtered using Millipore filters of pore size of 0.45μm.

2.7 Viscosity Measurements

Viscosity measurements of the micelle solution were made in an Ubbelohde viscometer, which was placed in a thermostatically controlled bath with a precision of ±0.1°C. The measurements were repeated at least three times and

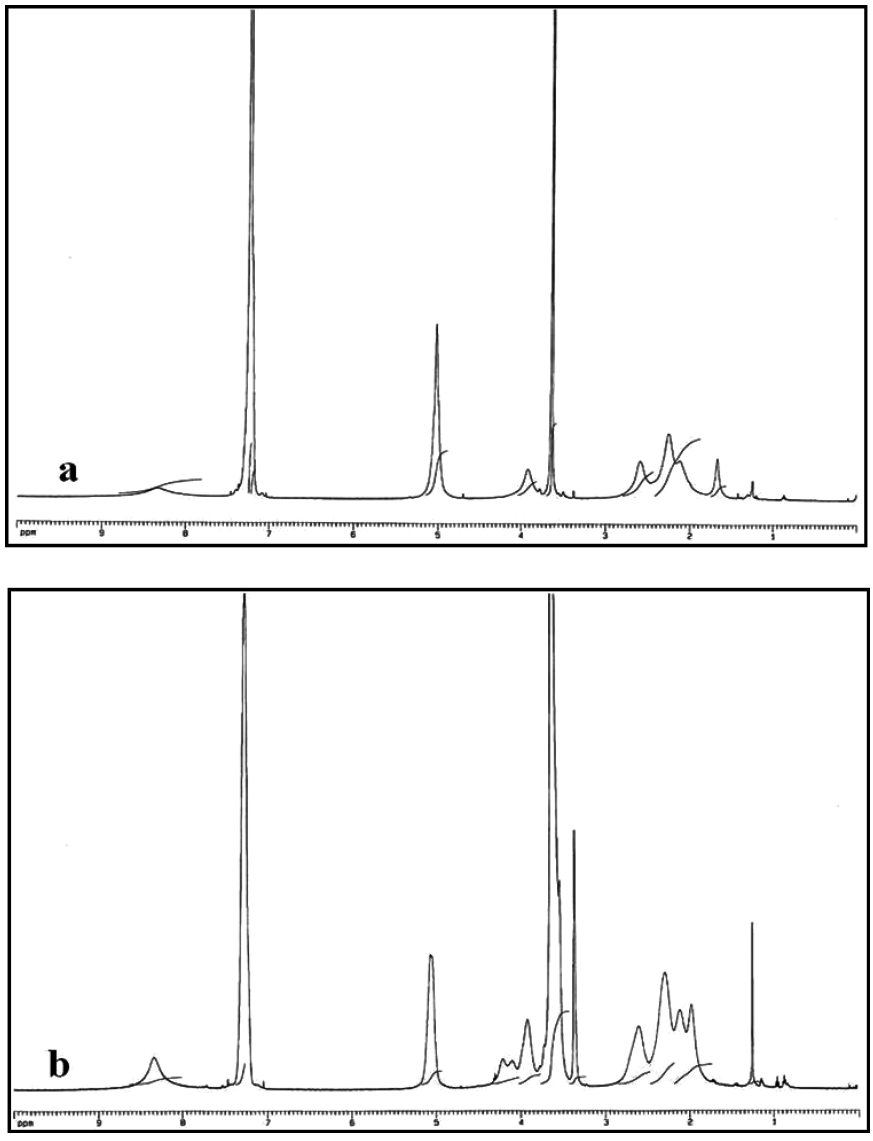

Fig. 3. ^{1}H-NMR spectra of (a) PBLG-*block*-PEG2 and (b) PEG-*b*-PBLG-*g*-PEG2 in $CDCl_3$.

the times obtained were arithmetically averaged, then converted to the relative viscosity (η_γ), η_γ was further converted to the specific viscosity (η_{sp}). The experiments were carried out by diluting the micelle solution step by step. The curve of η_{sp}/C vs. the concentration (C) of the micelle solution was drawn. By analyzing the curve of $\eta_{sp}/C \sim C$, the critical micelle concentration of polypeptide copolymers could be obtained (38).

3 Results and Discussion

3.1 ^{1}H-NMR Analysis

As mentioned above, the formation of PEG-*b*-PBLG-*g*-PEG2 copolymer could be demonstrated by the difference of the peak areas (3.62 ppm) in ^{1}H-NMR spectra of PBLG-*block*-PEG2 and PEG-*b*-PBLG-*g*-PEG2. Figure 3 presents the ^{1}H-NMR spectra of PBLG-*block*-PEG2 and PEG-*b*-PBLG-*g*-PEG2 in $CDCl_3$. As seen from Figure 3, for the two copolymers, the characteristic peaks appearing at 7.21 ppm and 5.11 ppm (corresponding to the phenyl protons in the PBLG segments and the methylene protons in the benzyl group of the PBLG segments, respectively) and the characteristic peak appearing at 3.62 ppm (corresponding to the ethylene protons of PEG segments) are detected (1,10). This phenomenon showed that both PBLG-*block*-PEG2 copolymer and PEG-*b*-PBLG-*g*-PEG2 copolymer are composed of PBLG and PEG components.

3.2 Observations of Transmission Electron Microscopy

Figure 4a and Figure 4b present the morphologies of the micelles formed by PBLG-*block*-PEG1 copolymer and

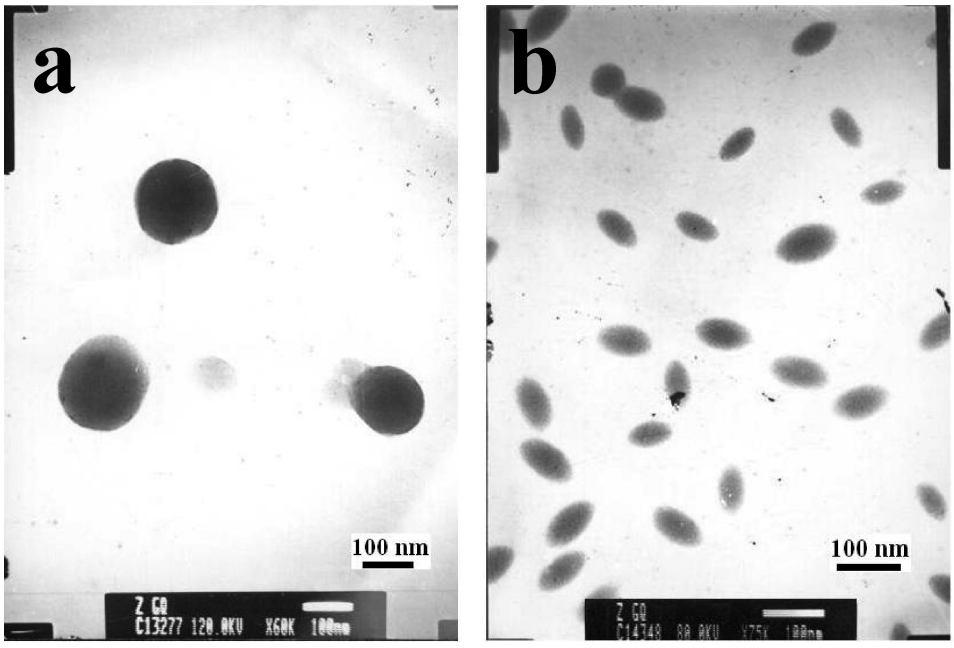

Fig. 4. TEM photographs of (a) the micelles formed by PBLG-*block*-PEG1 copolymer in ethanol and (b) the micelles formed by PEG-*b*-PBLG-*g*-PEG2 copolymer in ethanol.

PEG-*b*-PBLG-*g*-PEG2 copolymer in ethanol, respectively. As is shown in Figure 4, both PBLG-*block*-PEG1 copolymer and PEG-*b*-PBLG-*g*-PEG2 copolymer could self-assemble into polymeric micelles with the hydrophobic PBLG segments aggregating as the inner core of the micelles surrouded by the hydrophilic PEG chains. The morphology of the micelles with a core-shell structure formed by PBLG-*block*-PEG1 in ethanol is plump spherical shape, while the morphology of the micelles with a core-shell structure formed by PEG-*b*-PBLG-*g*-PEG2 in ethanol is regular rice-like shape. Compared with PBLG-*block*-PEG1 copolymer with pure block structure, PEG-*b*-PBLG-*g*-PEG2 copolymer holds both block structure and graft structure. As described in document (1), the difference in molecular architecture results in various morphologies of the micelles. This situation indicated that the different morphologies of the micelles formed by PBLG-*block*-PEG1 and PEG-*b*-PBLG-*g*-PEG2 in ethanol could be attributed to their different molecular structures.

3.3 Effects of the Introduction of PBLG Homopolymer on the Average Particle Diameter of the Micelles Based on PBLG-block-PEG and PEG-b-PBLG-g-PEG

Figure 5 presents the curves of the average particle diameter of the micelles formed by PBLG-block-PEG1 (shown by curve a) and PEG-b-PBLG-g-PEG2 (shown by curve b) versus the content (wt%) of PBLG homopolymer in the mixed system. As it can be seen from Figure 5, the average particle diameters of the micelles of both PBLG-block-PEG1 and PEG-b-PBLG-g-PEG2 increase with increasing the content of PBLG homopolymer in the mixed system. Due to the same hydrophobic property, PBLG homopolymer could self-assemble into polymeric micelles together with PBLG-*block*-PEG1 or PEG-*b*-PBLG-*g*-PEG2 through the interaction with PBLG chains of polypeptide copolymers. Also seen from Figure 5, the increasing degree of the average particle diameter of the micelles formed by PBLG-*block*-PEG1 is larger than that of the micelles formed by PEG-*b*-PBLG-*g*-PEG2. Due to the different molecular structures, the aggregating-resistance of PBLG

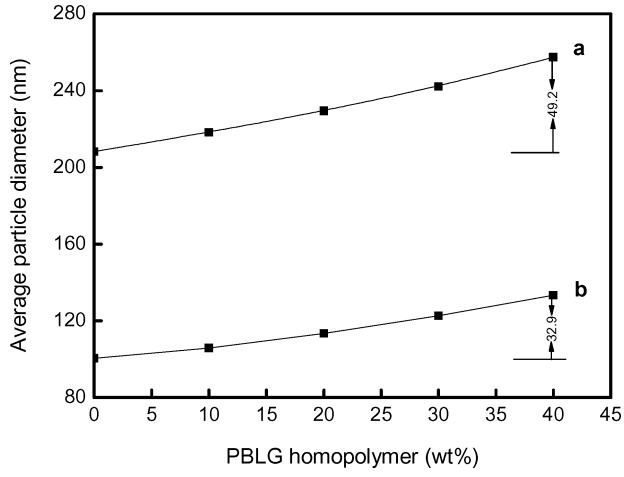

Fig. 5. Curves of the average particle diameter of the micelles formed by PBLG-*block*-PEG1 (shown by curve a) and PEG-*b*-PBLG-*g*-PEG2 (shown by curve b) versus the content (wt%) of PBLG homopolymer in the mixed system.

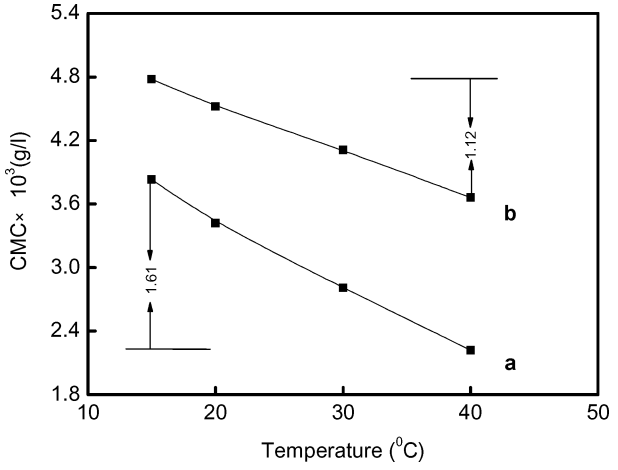

Fig. 6. Curves of the critical micelle concentration of PBLG-*block*-PEG1 (shown by curve a) and PEG-*b*-PBLG-*g*-PEG2 (shown by curve b) in ethanol vs. the testing temperature.

homopolymer with PBLG segments in PEG-*b*-PBLG-*g*-PEG2 is relatively bigger than that of PBLG homopolymer with PBLG segments in PBLG-*block*-PEG1, suggesting that the difference of the increasing degree of the average particle diameters of the micelles based on PBLG-*block*-PEG1 and PEG-*b*-PBLG-*g*-PEG2 could be attributed to their different molecular structures.

3.4 Effects of the Testing Temperature on the Critical Micelle Concentration of PBLG-block-PEG and PEG-b-PBLG-g-PEG

The critical micelle concentrations of PBLG-*block*-PEG1 and PEG-*b*-PBLG-*g*-PEG2 in ethanol were confirmed according to the document (38). Figure 6 shows the curves of the critical micelle concentration of PBLG-*block*-PEG1 (shown by curve a) and PEG-*b*-PBLG-*g*-PEG2 (shown by curve b) versus the testing temperature. As seen from Figure 6, the critical micelle concentrations of both PBLG-*block*-PEG1 and PEG-*b*-PBLG-*g*-PEG2 in ethanol decrease with the increase of the testing temperature. As described in the documents (38,39), the increase of the testing temperature promotes the interaction of PBLG segments in PBLG-*block*-PEG1 or in PEG-*b*-PBLG-*g*-PEG2 by accelerating the moving of polypeptide blocks, suggesting the critical micelle concentration decreases with the increase of the testing temperature. Also seen from Figure 6, the decreasing degree of the critical micelle concentration of PBLG-*block*-PEG1 is larger than that of PEG-*b*-PBLG-*g*-PEG2. Owing to the different molecular structures, the moving-resistance of PBLG segments in PEG-*b*-PBLG-*g*-PEG2 is relatively bigger than that of PBLG segments in PBLG-*block*-PEG1, indicating that their different molecular structures result in the difference of the decreasing degree of the critical micelle concentrations.

4 Conclusions

Poly(ethylene glycol)-*block*-poly(γ-benzyl *L*-glutamate)-*graft*-poly(ethylene glycol) copolymer and poly(γ-benzyl *L*-glutamate)-*block*-poly(ethylene glycol) copolymer have been synthesized. ^{1}H-NMR spectra were used to confirm the components of PEG-*b*-PBLG-*g*-PEG and PBLG-*block*-PEG. The self-assembly behaviors of PEG-*b*-PBLG-*g*-PEG and PBLG-*block*-PEG in ethanol were studied by TEM, DLS, and viscometry. ^{1}H-NMR measurements demonstrate that both PBLG-*block*-PEG and PEG-*b*-PBLG-*g*-PEG are composed of PBLG and PEG components. TEM observations prove that PBLG-*block*-PEG and PEG-*b*-PBLG-*g*-PEG could self-assemble to form polymeric micelles with a core-shell structure in the shapes of plump spherical and regular rice-like, respectively. DLS studies testify that the average particle diameters of the micelles of both PBLG-*block*-PEG and PEG-*b*-PBLG-*g*-PEG increase with the increase of PBLG homopolymer content in the mixed system, and the increasing degree of the average particle diameters of the micelles is different because of their different molecular structures. Viscosity measurements attest that the critical micelle concentrations of both PBLG-*block*-PEG and PEG-*b*-PBLG-*g*-PEG decrease with the increase of the testing temperature, and their different molecular structures result in the difference of the decreasing degree of the critical micelle concentrations.

Acknowledgements

The authors gratefully acknowledge the financial support granted by Shandong University of Technology.

References

1. Tang, D.M., Lin, J.P., Lin, S.L., Zhang, S.N., Chen, T. and Tian, X.H. (2004) *Macromol. Rapid Commun.*, 25, 1241–1246.
2. Gao, Z.S., Desjardins, A. and Eisenberg, A. (1992) *Macromolecules*, 25, 1300–1303.
3. Zhong, X.F., Varshney, S.K. and Eisenberg, A. (1992) *Macromolecules*, 25, 7160–7167.
4. Lin, J.P., Zhu, J.Q., Chen, T., Lin, S.L., Cai, C.H., Zhang, L.S., Zhuang, Y. and Wang, X.S. (2009) *Biomaterials*, 30, 108–117.
5. Lin, J.P., Zhang, S.N., Chen, T., Liu, C.S., Lin, S.L. and Tian, X.H. (2006) *J. Biomed. Mater. Res., Part B: Appl. Biomater.*, 76B, 432–439.
6. Harada, A., Cammas, S. and Kataoka, K. (1996) *Macromolecules*, 29, 6183–6188.
7. Moffitt, M. and Eisenberg, A. (1997) *Macromolecules*, 30, 4363–4373.
8. Lin, J.P., Liu, N., Chen, J. and Zhou, D.F. (2000) *Polymer*, 41, 6189–6194.
9. Lin, J.P. and Abe, A. (1996) *Macromolecules*, 29, 2584–2589.
10. Li, T., Lin, J.P., Chen, T. and Zhang, S.N. (2006) *Polymer*, 47, 4485–4489.
11. Zhang, L.S., Lin, J.P. and Lin, S.L. (2007) *Macromolecules*, 40, 5582–5592.
12. Lin, J.P., Ding, W.W., Hong, K.L., Mays, J.W., Xu, Z.D. and Yuan, Y.Z. (2008) *Soft Matter*, 4, 1605–1608.

13. Zhang, L.S., Lin, J.P. and Lin, S.L. (2007) *J. Phys. Chem. B*, 111, 351–357.
14. Zhang, L.S., Lin, J.P. and Lin, S.L. (2007) *J. Phys. Chem. B*, 111, 9209–9217.
15. Ding, W.W., Lin, S.L., Lin, J.P. and Zhang, L.S. (2008) *J. Phys. Chem. B*, 112, 776–783.
16. Xie, M.R., Kong, Y., Han, H.J., Shi, J.X., Ding, L., Song, C.M. and Zhang, Y.Q. (2008) *React. Funct. Polym.*, 68, 1601–1608.
17. Wei, Y.P., Cheng, F., Hou, G.L. and Sun, S.F. (2008) *React. Funct. Polym.*, 68, 981–989.
18. Zhang, S.G. and Altman, M. (1999) *React. Funct. Polym.*, 41, 91–102.
19. Zhang, Z.M., Wang, L.Q., Deng, J.Y. and Wan, M.X. (2008) *React. Funct. Polym.*, 68, 1081–1087.
20. Tikhonov, V.E., Stepnova, E.A., Babak, V.G., Krayukhina, M.A., Berezin, B.B. and Yamskov, I.A. (2008) *React. Funct. Polym.*, 68, 436–445.
21. Cho, C.S., Cheon, J.B., Jeong, Y.I., Kim, I.S., Kim, S.H. and Akaike, T. (1997) *Macromol. Rapid Commun.*, 18, 361–369.
22. Cho, C.S., Nah, J.W., Jeong, Y.I., Cheon, J.B., Asayama, S., Ise, H. and Akaike, T. (1999) *Polymer*, 40, 6769–6775.
23. Oh, I., Lee, K., Kwon, H.Y., Lee, Y.B., Shin, S.C., Cho, C.S. and Kim, C.K. (1999) *Int. J. Pharm.*, 181, 107–115.
24. Markland, P., Amidon, G.L. and Yang, V.C. (1999) *Int. J. Pharm.*, 178, 183–192.
25. Jeong, Y.I., Nah, J.W., Lee, H.C., Kim, S.H. and Cho, C.S. (1999) *Int. J. Pharm.*, 188, 49–58.
26. Kwon, G., Naito, M., Yokoyama, M., Okano, T., Sakurai, Y. and Kataoka, K. (1993) *Langmuir*, 9, 945–949.
27. Cheon, J.B., Jeong, Y.I. and Cho, C.S. (1999) *Polymer*, 40, 2041–2050.
28. Inomata, K., Ohara, N., Shimizu, H. and Nose, T. (1998) *Polymer*, 39, 3379–3386.
29. Inomata, K., Shimizu, H. and Nose, T. (2000) *J. Polym. Sci., Part B: Polym. Phys.*, 38, 1331–1340.
30. Watanaba, J., Ono, H., Uematsu, I. and Abe, A. (1985) *Macromolecules*, 18, 2141–2148.
31. Harada, A. and Kataoka, K. (1995) *Macromolecules*, 28, 5294–5299.
32. Lin, J.P., Zhang, S.N., Chen, T., Lin, S.L. and Jin, H.T. (2007) *Int. J. Pharm.*, 336, 49–57.
33. Lin, J.P., Zhu, G.Q., Zhu, X.M., Lin, S.L., Nose, T. and Ding, W.W. (2008) *Polymer*, 49, 1132–1136.
34. Chen, T., Lin, S.L., Lin, J.P. and Zhang, L.S. (2007) *Polymer*, 48, 2056–2063.
35. Liu, N. and Lin, J.P. (2001) *Polym. J.*, 33, 898–901.
36. Higashi, N., Kawahara, J. and Niwa, M. (2005) *J. Colloid Interf. Sci.*, 288, 83–87.
37. Zhang, W.Q., Shi, L.Q., An, Y.L., Wu, K., Gao, L.C. and Liu, Z. (2004) *Macromolecules*, 37, 2924–2929.
38. Xu, Z.S., Feng, L.X., Ji, J., Cheng, S.Y., Chen, Y.C. and Yi, C.F. (1998) *Eur. Polym. J.*, 34, 1499–1504.
39. Price, C., Kendall, K.D., Stubbersfield, R.B. and Wright, B. (1983) *Polym. Commun.*, 24, 326–328.
40. Nah, J.W., Jeong, Y.I. and Cho, C.S. (1998) *J. Polym. Sci., Part B: Polym. Phys.*, 36, 415–423.
41. Abe, A. and Yamazaki, T. (1989) *Macromolecules*, 22, 2138–2145.